

Impact of Local Histogram Equalization on Deep Learning architectures for Diagnosis of COVID-19 on Chest X-rays

1st Suleyman Serhan NARLI

*Department of Engineering and Natural Sciences
Iskenderun Technical University
Hatay, Turkey
ORCID: 0000-0003-0162-9786*

2nd Gokhan ALTAN

*Department of Engineering and Natural Sciences
Iskenderun Technical University
Hatay, Turkey
ORCID: 0000-0001-7883-3131*

Abstract—Deep Learning (DL) is one of the most popular Machine Learning (ML) algorithms with feature learning capabilities. Its use is becoming widespread day by day due to its high-performance in classification in the various fields, including medical image processing. DL is inspired by an advanced neural network structure and includes many parameters. In consequence of its high performance, it is used in the classification of many diseases. DL algorithms, which are frequently used in the field of image processing, classify the pixels on the images by convolutional progress in different layers. Before learning the significant pixels in supervised ways, it can be ensured that the classification is more successful with different preprocessing methods. In this study, the effect of DL architectures on COVID-19 was investigated using Local Histogram Equalization (LHE). Chest x-ray images were examined with- and without-LHE to determine the effect of disk factor on transfer learning. The dataset consists of COVID-19, pneumonia, and normal chest x-ray images. Chest x-rays were segmented into two parts as of right lung lobe and left lung lobe. The effect on classification performance of transfer learning was observed by applying different disk value for LHE. The experiments were evaluated on the different pre-trained DL architectures, such as VGG16, AlexNet, and Inception model.

Index Terms—Deep Learning, Convolutional Neural Networks, Chest X-Ray, Local Histogram Equalization, Medical Image Analysis.

I. INTRODUCTION

Image processing is the preparation of the image for classification and segmentation by applying advanced mathematical solutions and signal processing techniques. The image is generally considered by a two-dimensional matrix with three color channels (RGB-Red Green Blue) and each pixel in images is presented by a mathematical value between 0-255. Many algorithms for classification in image processing rely on the detection and extraction of local features in images. Conventional image processing tries to obtain the significance by characterizing the meaningful features in the image. Handcrafted method has been developed to solve the problem of feature extraction for classification. Afterwards, the elaborated handcrafted techniques used in classification and segmentation. However, applying pattern recognition systems with handcrafted techniques for large datasets is a challenging

process. There is no need to use handcrafted techniques in deep learning [1]; It uses many (deeper) unit layers with highly optimized algorithms, architectures, and regularizations. Feature learning and transfer learning, which are novel techniques in Deep Learning (DL), are used in the pattern recognition without a separate feature extraction stage. In conventional image processing techniques, Convolutional Neural Networks (CNN) has started to be used more than the handcrafted techniques, typical classifier deep neural networks, such as AlexNet [2], VGGNet [3] or GoogLeNet [4] are fed directly by images. The sequence in DL generates class probability. Whereas extracting the probabilistic prediction, the experiments are performed by using distinct datasets for training and validation. Generally, a CNN structure is formed as; The raw image is fed as input to the first layer of the network by allowing each layer to calculate its respective function on the output of the preceded layer. One of the most studied classification is handwritten number recognition, in which a neural network takes the image of a single handwritten digit. It must decide which of the ten digits are displayed on the images [5]. Deep learning has a widespread-use in a wide variety of machine learning tasks, including image classification, speech recognition, medical image processing, natural language processing, and more. There are many new researches on deep learning [6], [7], [8], [9], [10], [11], [12]. These studies examined deep learning techniques from different perspectives, with the applications of medical image analysis [13], natural language processing [14], speech recognition systems [10] and remote sensing [12]. Deep Neural Networks (DNN) consist of several layers of nodes, different architectures have been developed to solve various issues in different fields of use. Whereas the CNN is often used for computer vision and image recognition, recurrent neural network [15] is often used for time-series. The most common DNN architectures are this; 1) CNN, 2) Deep Autoencoders, 3) Long Short Term Memory (LSTM), 4) Restricted Boltzmann Machine (RBM). All these Deep architectures use backpropagation in the training stage of supervised learning. Backpropagation uses gradient-descent for error minimization, adjusting the weights according to the

partial derivative of the error function for each weight. Model training can be broadly divided into three types including supervised, unsupervised, and semi-supervised. Supervised learning uses labeled data to train the network, whereas unsupervised learning does not need labeled dataset. Accordingly, there is no feedback-based learning. In unsupervised learning, neural networks are pre-trained using manufacturing models such as RBMs and then fine-tuned using standard supervised learning algorithms on pre-trained weights. Afterwards, It is tested by a separate dataset to identify patterns or classification results. transfer learning is adapting the weights of a trained models for a different dataset. In DL, pruning is mainly used to developing a smaller and more efficient neural network model. The purposes of this technique are to optimize the model by eliminating the values of weight tensors and to obtain a less time consuming, computationally cost-effective model in training. Many studies have been performed in the field of medical image processing, such as CT images. 3-dimensional Deep architectures were used to automatically segment abdominal CT to identify arteries, portal veins, liver, spleen, stomach, gallbladder, and pancreas in each multi-organ image [16]. Deep convolution and deep belief networks, a type of RBM network, conditional random field, and structured support vector machine were utilized to separate breast masses from mammograms on mammograms [17]. Various methods were presented in the literature to detect pneumonia using chest X-ray images. Some of these methods use a machine learning algorithm as the classification technique and deep learning techniques for feature extraction and classification [18]. Similarly, [19] used logistic regression as a basic model for pneumonia detection using x-rays using a 121-layer dense convolutional network (DenseNet). In another study, Rajpurkar et al. developed a model that diagnoses pneumonia with a high accuracy rate, ChexNet developed a 121-layer CNN model that analyzes chest x-ray image and classified the image bilaterally and determined the probability of pneumonia [20]. Many studies were performed on DL-based medical image applications. Examples include SegNet [24], DenseU-Net [25] and CardiacNet [26], [27] in detecting pneumonia in CXRs. In this study, pre-processing was performed using the Local Histogram Equalization (LHE) method to make the tissues and masses in the lung images more visible before feeding the CNN for pathology detection on chest x-rays. Afterward, the performance of CNN and the effect of LHE with CNN on the detection of COVID-19, pneumonia, and normal images were evaluated. After LHE, it is aimed to increase the performance by combining similar tissues with CNN in the training stage. Lung images were cropped and separated as right and left lobe images, and only lung sections were inhaled. Thus, non-lung sections were eliminated from chest x-rays, and enabled the CNN architecture to be trained only on the lung sections for experimented architectures. The remaining of the paper is organized as follows. The CNN architecture, chest x-rays database, transfer learning on AlexNet, and LHE technique are detailed in Materials and Methods. The experimental setup and the achievements for various CNN architectures with-

without-LHE were presented and evaluated in experimental results. The advantages of the proposed technique, state-of-the-art, comparison considering various parameters with literature are evaluated and discussed in Discussion section.

II. MATERIALS AND METHODS

A. Convolutional Neural Networks

CNNs are a deep network model consisting of sequential convolutional layers and fully connected layers. The convolutional layers serve as feature extractors and learn the various representations of the input images. Output of convolutional layers are arranged in feature maps. Each neuron in a feature map has a receptive field that connects to a layer of neurons in the previous layer via a trainable set of weights [33]. Inputs are combined with learned weights to create a new feature map, and folded results are transferred via rectified linear units (ReLU) [32], which is a nonlinear activation function. The weights of each neuron in a feature map are equally constrained; however, different feature maps within the same convolution layer have different weights so that various features can be extracted at each location. The convolution layer consists of using various dimensions and numbers of filters to represent different properties of the inputs. The depth of the CNN is defined by the number of filters in each transform layer [?]. Deep learning models also include the pooling layer apart from the convolution layer, the purpose of this layer is to reduce the spatial resolution of the feature maps and thus achieve spatial invariance to enter distortions and translations. It is used to propagate the average of all values of a small region of an image to the next layer [33], [34]. After various numbers of sequential convolution layers and pool layers, the feature maps are stacked on top of each other, and the fully connected layers connected to flattened feature map. It interprets these layer representations and perform the classification function [35], [36]. It is standard to use the softmax function as output layer of fully connected layers [2].

B. Chest X-Ray Database

Chest x-ray images are a dataset obtained from real patients by chest x-ray examination and available in the clinical PACS database at the National Institutes of Health Clinical Center. The chest x-ray dataset includes 112,120 frontal view medical images of 30,805 unique patients with fourteen pulmonary diseases (each image can have multiple labels). Fourteen common thoracic pathologies are atelectasis, consolidation, infiltration, pneumothorax, edema, emphysema, fibrosis, effusion, pneumonia, pleural thickening, cardiomegaly, nodule, mass, and hernia [28]. This dataset is publicly available on the Kaggle platform¹. Similar datasets: Montgomery County X-ray Set [29], Shenzhen Hospital X-ray Set [29], ChexNet [20] etc. Pneumonia-diagnosed lung images and healthy lung images were selected from the NIH Chest X-Ray dataset. The chest x-rays with COVID-19 were selected from the COVIDx dataset. This dataset is the largest open-access dataset in terms

¹<https://www.kaggle.com/nih-chest-xrays/data>

of the number of COVID-19 positive patient cases². Many datasets are also publicly available in [21], [22], [23]. Chest x-ray can show areas such as edema, nodule, and infiltration in the lungs according to different intensity colors, making diagnosis difficult in the early stages due to the noisy image. In such cases, thanks to the filters applied on the image and by localizing the lung regions by segmentation on the images, the noise can be reduced by selecting certain regions and the performance of the dataset trained with deep learning can be increased. When we examine the publications in this area, the medical images can be processed with machine learning methods and the diagnosis of pathology for many lung diseases can be performed with the sensitivity of the doctor. Automatized techniques can also play an important role in identifying many pathologies and for early diagnosis with the enhancements of DL algorithms and architectures.

C. AlexNet and Transfer Learning

AlexNet is a DL architecture created by Alex Krizhevsky et al. [2] for ImageNet large visual recognition in 2012. It is a basic, simple, and an effective CNN architecture consisting mainly of gradual stages such as convolution layers, pool layers, corrected linear unit (ReLU). Specifically, AlexNet has five convolutional layers: first layer, second layer, third layer, and fourth layer, followed by pool layer and fifth layer, then three fully connected layers, respectively [2]. In this study, transfer learning was applied using the AlexNet architecture and the chest x-ray images were classified into multi classes. Transfer learning is a method of retraining a pre-trained model on a new dataset. The model is applied to the new dataset by fine-tuning the model in transfer learning. In this study, we adapted transfer learning into the chest x-ray database using the AlexNet architecture. The number of filters in the convolution layers of the model was reduced by pruning, thus performance improvement was reported on pruned AlexNet architecture. Since AlexNet architecture is a model created for a large dataset, it is well-adapted to the experimented small-scale dataset. The AlexNet architecture was pruned and supervised stage was trained using a single full connected layer instead of the last three fully connected layers. Thus, it was ensured that there was not much cohesion in the training of the model. The proposed architecture is depicted in Figure(2).

D. Local Histogram Equalization

Automatic contrast enhancement is one of the common operations performed on visual data to reveal confidential detail. A histogram is a graph showing pixel density. Global histogram equalization (GHE) is generally a global tone mapping process, allowing the gray level of each pixel to be recreated by calculating the overall histogram of the image. However, these processes fail to increase contrast in both dark and bright image regions at the same time. Especially, small bright spots are hardly visible after such a global operation. To solve this problem, local histogram equalization (LHE) was

proposed to perform in a floating window with this adjustable window size (radius or disk). Histogram equalization is applied independently to small areas of the image, thus preserving the contrast adjustment for different regions of the image [37], [38], [39]. In this study, chest x-ray images were preprocessed using LHE. Figure(1) indicates the lung images for different LHE window sizes (disk) values.

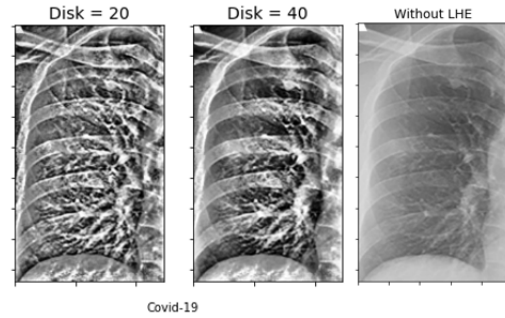


Fig. 1. Different LHE (disk) values

III. EXPERIMENTAL RESULTS

AlexNet architecture was proposed by Alex Krizhevsky et al. in 2012. The total data size in this study consists of 2856 images for each model training, which is very small-scale dataset for the AlexNet architecture. Therefore, while the data is adapted to the AlexNet architecture with transfer learning, the number of filters in the convolution layers has been changed and the model has been optimized according to the training performance. By cropping the chest x-ray images, 2 lung lobes were cropped from each chest x-ray, separately. Thus, 1000 healthy lung images, 1000 lung images diagnosed with Pneumonia, and finally 856 lung images diagnosed with COVID-19 were experimented in the analysis. Two floating window parameters (disk) were used for LHE with 20 and 40. The model has been optimized by fine-tuning the parameters on the AlexNet model. Instead of the last three fully connected layers in the AlexNet architecture, one fully connected layer is used, thus we prevented overfitting and reducing the number of the classification parameters. As in the AlexNet architecture, 5 convolution layers were used in the pruned model and the number of filters for each layer are determined in this way for 32, 64, 128, 256 and 512, respectively. The dataset is split into three folds with 20%, 20%, and 60% for model testing, validation, and training, respectively. The batch size is 32 and the epoch number is 50 in the training of the fully connected layers. An early stopping was used to prevent overfitting during the supervised learning. In the last layer, 3 multi-classes are used for classification using the softmax function (COVID-19, Pneumonia, and Normal). We set $0.85e*5$ for the learning rate in the adam optimizer. In this manner, the hyper-parameters in the model were arranged. The total number of classification parameters was 2,072,899. Tensorflow framework with python programming language was chosen to train the model (GPU: Nvidia Rtx 2060).

²www.kaggle.com/tawsifurrahman/covid19-radiography-database

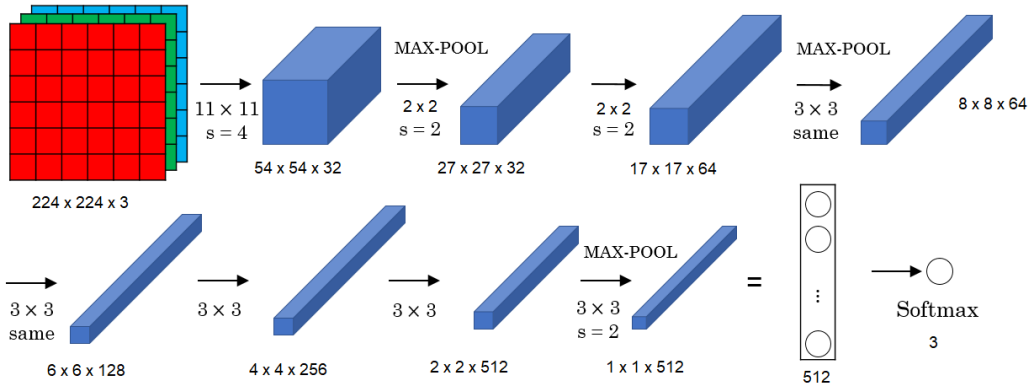


Fig. 2. The proposed pruned AlexNet architecture.

We calculated accuracy, precision, recall, and f1 Score were used to evaluate the performance of the model. The accuracy of a test is the ability to accurately distinguish patient and healthy cases. It is the calculation of the ratio of true positive and true negative in each case. Recall, the sensitivity of a test is its ability to accurately identify patient cases. It is the metric of the true positive rate in diseased cases. Precision is the metric to test the models's ability to accurately identify healthy cases, and calculate the true negative rate in healthy cases. Confusion Matrix results for different LHE Disk values are presented in Table I.

$$OverallAccuracy = \frac{TP + TN}{TP + TN + FP + FN} \quad (1)$$

$$Recall = \frac{TP}{TP + FN} \quad (2)$$

$$Precision = \frac{TP}{TP + FP} \quad (3)$$

$$F1score = \frac{2TP}{2TP + FP + FN} \quad (4)$$

True positive (TP), number of cases correctly identified patients; false positive (FP), number of cases incorrectly identified as patients; true negative (TN), the number of cases correctly identified as healthy; and the number of false-negative (FN) cases incorrectly identified as healthy.

TABLE I
CONFUSION MATRIX RESULTS FOR DIFFERENT LHE DISK VALUES

| | Confusion Matrix | Normal | Pneumonia | Covid-19 |
|------------------------|------------------|--------|-----------|----------|
| Without LHE | Normal | 170 | 3 | 7 |
| | Pneumonia | 4 | 200 | 1 |
| | Covid-19 | 25 | 10 | 150 |
| LHE (disk = 20) | Normal | 150 | 8 | 24 |
| | Pneumonia | 0 | 190 | 20 |
| | Covid-19 | 18 | 14 | 150 |
| LHE (disk = 40) | Normal | 160 | 6 | 13 |
| | Pneumonia | 0 | 200 | 5 |
| | Covid-19 | 15 | 4 | 160 |

A. Discussion

COVID-19 analysis of many researching areas has gained importance to ease the diagnosis and detection rate of disease for a pandemic. Consequently, advancing image processing techniques and proposing robust CADx systems are the main focus of researchers. The manuscripts for assessments of COVID-19 and using automatized techniques for abnormality detection within various diagnostic tools indicate the popularity of the field in 2020. Whereas high classification performances for diagnosis of COVID-19 were reported using Deep models with complex Deep learning architectures, applying simple pre-processing stages to the evaluation process reached high enough achievements using pruned and simple Deep architectures. The main ideas are using the generated representations instead of many convolutional layers, transmitting feature learning within resembled instances with LHE, and adapting the capability of feature transferring between adjacent layers for identification of chest x-rays with healthy, COVID-19, and pneumonia pathology.

TABLE II
COMPARISON OF RELEVANT DL-BASED DISEASE CLASSIFICATION STUDIES IN TERMS OF DIFFERENT DISK VALUES FOR LHE

| Disk Value | Data(Train/Test) | Accuracy | Precision | Recall | F1 Score |
|--------------------|------------------|----------|-----------|--------|----------|
| Without LHE | 2284/572 | 91% | 91% | 91% | 91% |
| 20 | 2284/572 | 85% | 85% | 85% | 85% |
| 40 | 2284/572 | 92% | 92% | 92% | 92% |

Table III presents the comparison of our study with the deep learning algorithms developed for the diagnosis of COVID-19. Wang et al. reported an accuracy rate of 93.3% for their proposed COVID-Net model using cropping, translation, rotation, horizontal rotation, zoom on chest x-rays [40]. Karthik et al. proposed a different deep learning model to learn specific filters within a single convolutional layer to identify specific classes of pneumonia. Their proposal achieved an F1 score rate of 97.20% for 112 chest x-rays with COVID-19. Moreover, the lung regions were divided into sections by applying a pre-trained algorithm and the segmentation process was applied [41]. Ozturk et al. presented the DarkNet model, which is a

TABLE III
COMPARISON OF RELEVANT DL-BASED COVID-19 DISEASE DETECTION STUDIES IN TERMS OF ALGORITHMS AND PERFORMANCES

| Related Works | Methods | Classifier | Covid-19 Test Sample | ACC (%) | F1 Score (%) | F1-score for COVID-19 (%) |
|-------------------------------|--|------------|-------------------------|---------|--------------|------------------------------------|
| Wang et al. [40] | COVID-Net CNN | CNN | 100 | 93.3 | 93.13 | 94.78 |
| Karthik et al. [41] | Customized CNN with distinctive filter learning module | CNN | 112 | 97.94 | 96.90 | 97.20 |
| Ozturk et al. [42] | DarkNet-19 | CNN | 25 | 87.02 | 88.0 | 88 |
| Khan et al. [43] | CoroNet net | CNN | 70 | 89.6 | 89.8 | 95.61 |
| Apostolopoulos et al. [44] | Transfer learning with MobileNetV2 | CNN | 222 | 94.72 | 93.80 | 90.50 |
| Farooq et al. [45] | Transfer learning with ResNet50 | CNN | 68 | 96.23 | 96.88 | 100 |
| Hemdan et al. [46] | COVIDX-Net | CNN | 25 | 90 | - | - |
| Narin et al. [47] | ResNet-50 | CNN | 100 | 98 | - | - |
| Our Study | AlexNet Model without LHE | CNN | 572 | 91 | 91 | 87 |
| Our Study | AlexNet Model With LHE Disk 20 | CNN | 572 | 85 | 85 | 80 |
| Our Study | AlexNet Model With LHE Disk 40 | CNN | 572 | 92 | 92 | 90 |

novel model for the detection of COVID-19 which consists of 17 convolutional layers for binary classification(COVID-19 and no finding), and multi-class classification (no finding, COVID-19, and pneumonia). The model achieved the classification accuracy rates of 98.08% and 87.02% for binary classification and multi-class classification [42]. Khan et al. reported the CoroNet model, which is based on the pre-trained Xception CNN architecture and achieved classification accuracy of 95% for 3 classes (COVID-19, pneumonia, and normal) [43]. Apostolopoulos et al. reached an accuracy rate of 96.78% using transfer learning on MobileNetV2 [44]. Farooq et al. developed the COVID-ResNet model by fine-tuning the ResNet50 model and with transfer learning and achieved an accuracy rate of 96.23% in the COVIDx dataset [45]. Hemdan et al. proposed a novel model COVIDX-Net that is based on seven different architectures of DCNNs; VGG19, DenseNet201, InceptionV3, ResNetV2, InceptionResNetV2, Xception, and MobileNetV2. They reported performance rate range for various pre-tained architectures between 80-90% [46]. Narin et al. evaluated five pre-trained convolutional neural network-based models including ResNet50, ResNet101, ResNet152, InceptionV3 and Inception-ResNetV2. He applied three different binary classifications with four classes (COVID-19, normal (healthy), viral pneumonia, and bacterial pneumonia) using 5-fold cross-validation. Among the other four models used, the pre-trained ResNet50 model had the highest classification performance for different datasets with accuracy rate of 99.5% [47]. The state-of-the-art indicates that the pre-trained CNN architectures, pruned net-works, and using detailed feature learning stages can separate COVID-19 from healthy and pneumonia. Using hybrid methods in resembling stage of deep architectures, pruning the complex pre-trained architectures with transfer learning, and proposing light-weight architectures with simplistic image processing approaches can

advance the deep models. The proposed pruned CNN architecture with LHE is a powerful trajectory to get high enough results with easy-adaptable real-time applications over to the state-of-art. The proposed model possesses the capabilities of pre-trained detailed CNN architectures by feeding the input with resembled chest X-rays before the layer-wise feature learning. Using LHE for generating smoothed representation provided high enough classification performances using pruned AlexNet architecture. Therefore, simplifying the deep architectures enables reducing the training time of the COVID-19 identification architectures and integrating the shallow architectures for even real-time applications in embedded systems.

B. Conclusion

The study contains the novelty of applying LHE for generating resembling representations for increasing the generalization capability of CNN with shallow architectures. Whereas many studies are focusing on just classification performances in supervised training and modeling feature learning stages, the proposal is a pioneer study with LHE, which has a common use on medical images. The necessity of big data for the training of CNN architectures is overcome using LHE as a resembling procedure using a middle-scale chest x-ray dataset. The proposed model has reached high identification rates for multi-class diseases using is a basic, pruned architecture. It is easy-to-integrate architecture for various types of medical image analysis. Using novel visualization techniques and localization algorithms on chest x-rays has a possible contribution to Deep Learning algorithms. Although CNN architectures don't need additional feature extraction and pre-processing procedures, it has limitations in detecting small pathologies with low generalization capabilities. In the view that the classification assignments for modeling

architectures in CNN limited the variance in the COVID-19 analysis on chest x-rays, feeding the architectures with generative representations is a novel approach for minimizing the loss, increasing the performance for even shallow models. In further analysis, evaluating various localization parameters and experimenting with various lightweight architectures will enhance the performance capabilities on both left, right, and both lungs, separately.

REFERENCES

- [1] Lowe, D.G. Distinctive Image Features from Scale-Invariant Key-points. *International Journal of Computer Vision* 60, 91–110 (2004). <https://doi.org/10.1023/B:VISI.0000029664.99615.94>.
- [2] A. Krizhevsky, I. Sutskever, and G. E. Hinton. Imagenet classification with deep convolutional neural networks. In *NIPS*, 2012.
- [3] K. Simonyan and A. Zisserman. Very deep convolutional networks for large-scale image recognition. 2015, arXiv:1409.1556v6 [cs.CV].
- [4] C. Szegedy, W. Liu, Y. Jia, et al. Going deeper with convolutions. In *2015 IEEE Conference on Computer Vision and Pattern Recognition*, pages 1–9, 2015.
- [5] H. Li, R. Zhao, and X. Wang. Highly efficient forward and backward propagation of convolutional neural networks for pixelwise classification. 2014, arXiv:1412.4526v2 [cs.CV].
- [6] Goodfellow, I., Bengio, Y., Courville, A. (2016). *Deep learning*. Cambridge: MIT press.
- [7] LeCun, Y., Bengio, Y., Hinton, G. (2015). *Deep learning*. *Nature*, 521, 436–444.
- [8] Pouyanfar, S., Sadiq, S., Yan, Y., Tian, H., Tao, Y., Reyes, M. P., et al. (2018). A survey on deep learning: Algorithms, techniques, and applications. *ACM Computing Surveys*, 51(5), 92:1–92:36.
- [9] Wu, Z., Pan, S., Chen, F., Long, G., Zhang, C., Yu, P. S. (2019). A comprehensive survey on graph neural networks. arXiv:1901.00596.
- [10] Zhang, Z., Geiger, J., Pohjalainen, J., Mousa, A. E., Jin, W., Schuller, B. (2018d). Deep learning for environmentally robust speech recognition: An overview of recent developments. *ACM Transactions on Intelligent Systems and Technology*, 9(5), 49:1–49:28.
- [11] Zhou, J., Cui, G., Zhang, Z., Yang, C., Liu, Z., Sun, M. (2018a). Graph neural networks: A review of methods and applications. arXiv:1812.08434.
- [12] Zhu, X., Tuia, D., Mou, L., Xia, G., Zhang, L., Xu, F., et al. (2017). Deep learning in remote sensing: A comprehensive review and list of resources. *IEEE Geoscience and Remote Sensing Magazine*, 5(4), 8–36.
- [13] Litjens, G., Kooi, T., Bejnordi, B., Setio, A., Ciompi, F., Ghafoorian, M., et al. (2017). A survey on deep learning in medical image analysis. *Medical Image Analysis*, 42, 60–88.
- [14] Young, T., Hazarika, D., Poria, S., Cambria, E. (2018). Recent trends in deep learning based natural language processing. *IEEE Computational Intelligence Magazine*, 13(3), 55–75.
- [15] K. Cho. (2014). “Learning phrase representations using RNN encoderdecoder for statistical machine translation.” [Online]. Available: <https://arxiv.org/abs/1406.1078>
- [16] H.R. Roth, et al. Deep learning and its application to medical image segmentation (2018), pp. 1-6
- [17] Deep learning and structured prediction for the segmentation of mass in mammograms, N. Navab, J. Hornegger, W. Wells, A. Frangi (Eds.), *Medical image computing and computer-assisted intervention – MICCAI 2015*. MICCAI 2015. Lecture notes in computer science, vol. 9349 (2015), pp. 605-612
- [18] Luján-García, J.E.; Yáñez-Márquez, C.; Villuendas-Rey, Y.; Camacho-Nieto, O. A Transfer Learning Method for Pneumonia Classification and Visualization. *Appl. Sci.* 2020, 10, 2908.
- [19] Antin, B.; Kravitz, J.; Martayan, E. Detecting Pneumonia in Chest X-rays with Supervised Learning; Semanticscholar Org.: Allen Institute for Artificial intelligence, Seattle, WA, USA, 2017.
- [20] Rajpurkar, P.; Irvin, J.; Zhu, K.; Yang, B.; Mehta, H.; Duan, T.; Ding, D.; Bagul, A.; Langlotz, C.; Shpanskaya, K.; et al. Chexnet: Radiologist-level pneumonia detection on chest x-rays with deep learning. arXiv 2017, arXiv:1711.05225.
- [21] Cohen, J. P., Morrison, P., Dao, L. COVID-19 image data collection. arXiv:2003.11597 (2020).
- [22] Chung, A. Figure 1 COVID-19 chest x-ray data initiative. <https://github.com/agchung/Figure1-COVID-chestxray-dataset> (2020).
- [23] Radiological Society of North America. COVID-19 radiography database. <https://www.kaggle.com/tawsifurrahman/covid19-radiography-database> (2019).
- [24] V. Badrinarayanan, A. Kendall, and R. Cipolla, “SegNet: A Deep Convolutional Encoder-Decoder Architecture for Image Segmentation,” *IEEE Trans. Pattern Anal. Mach. Intell.*, vol. 39, no. 12, pp. 2481–2495, Dec. 2017, doi: 10.1109/TPAMI.2016.2644615.
- [25] X. Li, H. Chen, X. Qi, Q. Dou, C. W. Fu, and P. A. Heng, “HDenseUNet: Hybrid Densely Connected UNet for Liver and Tumor Segmentation from CT Volumes,” *IEEE Trans. Med. Imaging*, vol. 37, no. 12, pp. 2663–2674, Dec. 2018, doi: 10.1109/TMI.2018.2845918.
- [26] A. Mortazi, R. Karim, K. Rhode, J. Burt, and U. Bagci, “CardiacNET: Segmentation of left atrium and proximal pulmonary veins from MRI using multi-view CNN,” in *Lecture Notes in Computer Science (including subseries Lecture Notes in Artificial Intelligence and Lecture Notes in Bioinformatics)*, 2017, vol. 10434 LNCS, pp. 377–385, doi: 10.1007/978-3-319-66185-8-43.
- [27] I. M. Baltruschat, H. Nickisch, M. Grass, T. Knopp, and A. Saalbach, “Comparison of Deep Learning Approaches for Multi-Label Chest X-Ray Classification,” *Sci. Rep.*, vol. 9, no. 1, pp. 1–10, Dec. 2019, doi: 10.1038/s41598-019-42294-8.
- [28] Xiaosong Wang, Yifan Peng, Le Lu, Zhiyong Lu, Mohammad-hadi Bagheri, Ronald Summers, ChestX-ray8: Hospital-scale Chest X-ray Database and Benchmarks on Weakly-Supervised Classification and Localization of Common Thorax Diseases, *IEEE CVPR*, pp. 3462-3471, 2017
- [29] Jaeger S, Candemir S, Antani S, Wáng YX, Lu PX, Thoma G. Two public chest X-ray datasets for computer-aided screening of pulmonary diseases. *Quant Imaging Med Surg.* 2014 Dec;4(6):475-7. doi: 10.3978/j.issn.2223-4292.2014.11.20. PMID: 25525580; PMCID: PMC4256233.
- [30] Roosa K, Lee Y, Luo R, Kirpich A, Rothenberg R, Hyman JM, and et al. Real-time forecasts of the COVID-19 epidemic in China from February 5th to February 24th, 2020. *Infectious Disease Modelling*, 5:256-263, 2020.
- [31] Coronavirus. World Health Organization: <https://www.who.int/healthtopics/coronavirus,2020>.
- [32] Nair, V., Hinton, G. E. (2010). Rectified linear units improve restricted Boltzmann machines. In *Proceedings of the 27th International Conference on Machine Learning* (pp. 807–814). N.p.: International Machine Learning Society.
- [33] LeCun, Y., Bengio, Y., Hinton, G. (2015). *Deep learning*. *Nature*, 521(7553), 436–444.
- [34] Ranzato, M. A., Huang, F. J., Boureau, Y., LeCun, Y. (2007). Unsupervised learning of invariant feature hierarchies with applications to object recognition. In *Proceedings IEEE Conference on Computer Vision and Pattern Recognition* (pp. 1–8). Los Alamitos, CA: IEEE Computer Society.
- [35] Hinton, G. E., Srivastava, N., Krizhevsky, A., Sutskever, I., Salakhutdinov, R. R. (2012). Improving neural networks by preventing co-adaptation of feature detectors. arXiv 1207.0580.
- [36] Zeiler, M. D., Fergus, R. (2014). Visualizing and understanding convolutional networks. In *Proceedings of the European Conference on Computer Vision* (pp. 818–833). Berlin: Springer.
- [37] *Digital Image Processing-Concepts, Algorithms, and Scientific Applications*, Jaehne. B, Springer, Berlin 1991.
- [38] V. Caselles, J. L. Lisani, J. M. Morel, and G. Sapiro, “Shape preserving local histogram modification,” *IEEE Trans image proc*, vol. 8, no. 2, pp. 220-230, Feb. 1999.
- [39] J. Y. Kim, L. S. Kim, and S. H. Hwang, “An advanced contrast enhancement using partially overlapped sub-block histogram equalization,” *IEEE Trans circuits systems and video technology*, vol. 11, no. 4, pp. 475-484, Apr. 2001.
- [40] Wang, L., Lin, Z.Q. Wong, A. COVID-Net: a tailored deep convolutional neural network design for detection of COVID-19 cases from chest X-ray images. *Sci Rep* 10, 19549 (2020). <https://doi.org/10.1038/s41598-020-76550-z>.
- [41] Karthik R, Menaka R, M H. Learning distinctive filters for COVID-19 detection from chest X-ray using shuffled residual CNN. *Appl Soft Comput.* 2021;99:106744. doi:10.1016/j.asoc.2020.106744.

- [42] Ozturk T., Talo M., Yildirim E.A., Baloglu U.B., Yildirim O., Rajendra Acharya U. Automated detection of COVID-19 cases using deep neural networks with X-ray images. *Comput. Biol. Med.* 2020;121.
- [43] Khan A.I., Shah J.L., Bhat M.M. Coronet: A deep neural network for detection and diagnosis of COVID-19 from chest x-ray images. *Comput. Methods Programs Biomed.* 2020.
- [44] Apostolopoulos I.D., Mpesiana T.A. Covid-19: automatic detection from X-ray images utilizing transfer learning with convolutional neural networks. *Phys. Eng. Sci. Med.* 2020.
- [45] Farooq Muhammad, Hafeez Abdul. 2020. Covid-resnet: a deep learning framework for screening of covid19 from radiograph. *arXiv preprint arXiv:2003.14395*.
- [46] Hemdan E.E.-D., Shouman M.A., Karar M.E. COVIDX-Net: A framework of deep learning classifiers to diagnose covid-19 in X-ray images (2020) *arXiv preprint arXiv:2003.11055*.
- [47] Narin A., Kaya C., Pamuk Z. Automatic detection of coronavirus disease (COVID-19) using X-ray images and deep convolutional neural networks (2020).